Case Studies in Construction Materials 19 (2023) e02225

Contents lists available at ScienceDirect

Case Studies in Construction Materials

journal homepage: www.elsevier.com/locate/cscm

Building materials and decay assessment of the Gerace Cathedral (Reggio Calabria, Southern Italy)

Michela Ricca [a], Antonio Donato [a,*], Martina Cirone [a], Silvestro Antonio Ruffolo [a,*], Antonio Costanzo [b], Fabrizia Buongiorno [c], Giuseppe Mantella [d], Mauro Francesco La Russa [a], Luciana Randazzo [e]

[a] University of Calabria, Department of Biology, Ecology and Earth Sciences, Via P. Bucci, Cubo 12B, 87036 Arcavacata di Rende (CS), Italy
[b] National Earthquake Observatory, Istituto Nazionale di Geofisica e Vulcanologia, 87036 Rende, Italy
[c] National Earthquake Observatory, Istituto Nazionale di Geofisica e Vulcanologia, 00143 Roma, Italy
[d] Giuseppe Mantella Restauro Opere D'Arte, Circonvallazione Paparo 25, 88060 Isca sullo Ionio, Italy
[e] University of Palermo, Department of Earth and Marine Sciences, Via Archirafi, 26, 90123 Palermo, Italy

ARTICLE INFO

Keywords:
Diagnostic
Gerace cathedral
Stone materials
Pigments
Plasters
Restoration

ABSTRACT

A multi-analytical approach was employed for the first time to study the stone materials, wall paintings and related degradation forms in the Cathedral of Gerace (Reggio Calabria, southern Italy). With an area of around 1898 square meters, the Gerace Cathedral is the largest in Calabria: its construction dates back to the Norman era (between 1085 and 1120), and currently displays distinct features of Greek and Latin architectural orders. Despite having undergone numerous restorations, the church perfectly preserves its original buildings materials. Following an extensive site inspection campaign, supported by the experts dealing with building restoration, several areas were selected for analyses. Both in situ investigations and laboratory tests were carried out on micro-fragments using Non-Destructive and Micro-Destructive Techniques (NDTs and MDTs). The first step involved an inspection through InfraRed Thermography (IRT) in order to map the internal walls of the Cathedral and identify zones with potential degradation phenomena. Subsequently, a more in-depth study was designed based on the thermographic results, and laboratory tests were carried out on micro-fragments and powders to characterize the different kinds of materials (i.e., stones, mortars, plasters and pigments) and decay agents (i.e., salts and efflorescences). Thirty-one samples were subjected to a complementary analytical approach which included Polarizing Optical Microscopy (POM), Ion Chromatography (IC), X-Ray Powder Diffraction (XRPD) and Scanning Electron Microscopy (SEM) coupled with microanalysis (EDS). The results allowed us to preliminarily characterize the different materials from which the Cathedral was built, determine its state of conservation and provide a better knowledge of the entire building, revealing details not visible to the naked eye which are important for future conservation interventions. As for the state of conservation, the integrated use of various techniques enabled the detection of rising damp generally correlated with the occurrence of water infiltration and migration phenomena which appear to affect a large part of the building, causing noticeable damage (i.e., loss of surface material, micro-cracks, white salt efflorescence, etc.). The characterization of the materials carried out on mortars, plasters, and pigments also confirmed the local origin of the raw materials. However, the provenance of the studied marbles and

* Corresponding authors.
E-mail addresses: antonio.donato93@unical.it (A. Donato), silvestro.ruffolo@unical.it (S.A. Ruffolo).

https://doi.org/10.1016/j.cscm.2023.e02225
Received 31 March 2023; Received in revised form 17 May 2023; Accepted 18 June 2023
Available online 19 June 2023

crystalline limestones, could not be established and, therefore, further in-depth studies are required.

1. Introduction and historical background

The degradation of cultural heritage materials represents one of the most prominent threats to their preservation. During their useful life, materials are commonly subjected to degradation processes through their exposure to specific environmental conditions as well as chemical, physical, and biological phenomena. Hence, ageing is a critical factor in the durability and use of building materials which can lead to irreversible losses if not addressed in time [1–6]. In such a context, the scientific community generally encourages interdisciplinary research to implement new conservation and protection strategies for preserving cultural heritage. Current research [1–6] illustrates that in order to study the decay of building materials and perform effective restoration interventions, a cohesive, holistic, and multidisciplinary approach is needed which includes the historical, archeological, and architectural documentation, environmental monitoring, and evaluation and characterization of materials, as well as a knowledge of any previous interventions. To achieve this goal, the scientific community can use both Non-Destructive (NDTs) and Micro-Destructive Techniques (MDTs) which are useful for the characterization of building materials and the determination of the pathologies affecting a monument [1,2].

This paper presents the case study of the Cathedral of Gerace (Italy). The study deals with the decay affecting some building materials and provide an in-depth scientific survey performed to understand and demonstrate the causes of deterioration.

The Cathedral of Gerace, dedicated to Santa Maria Assunta (Fig. 1), was probably built between the second half of the penultimate decade of the 11th century and the first years of the 12th century on the remains of a pre-existing sacred building devoted to Aghìa Kyriakì (Saint Ciriaca) dating back to 7th-8th century [7]. It was then completed around the 4th decade of the 12th century under the Normans rule [8,9]. Due to numerous earthquakes which strongly damaged the historic center of Gerace, such as that of central

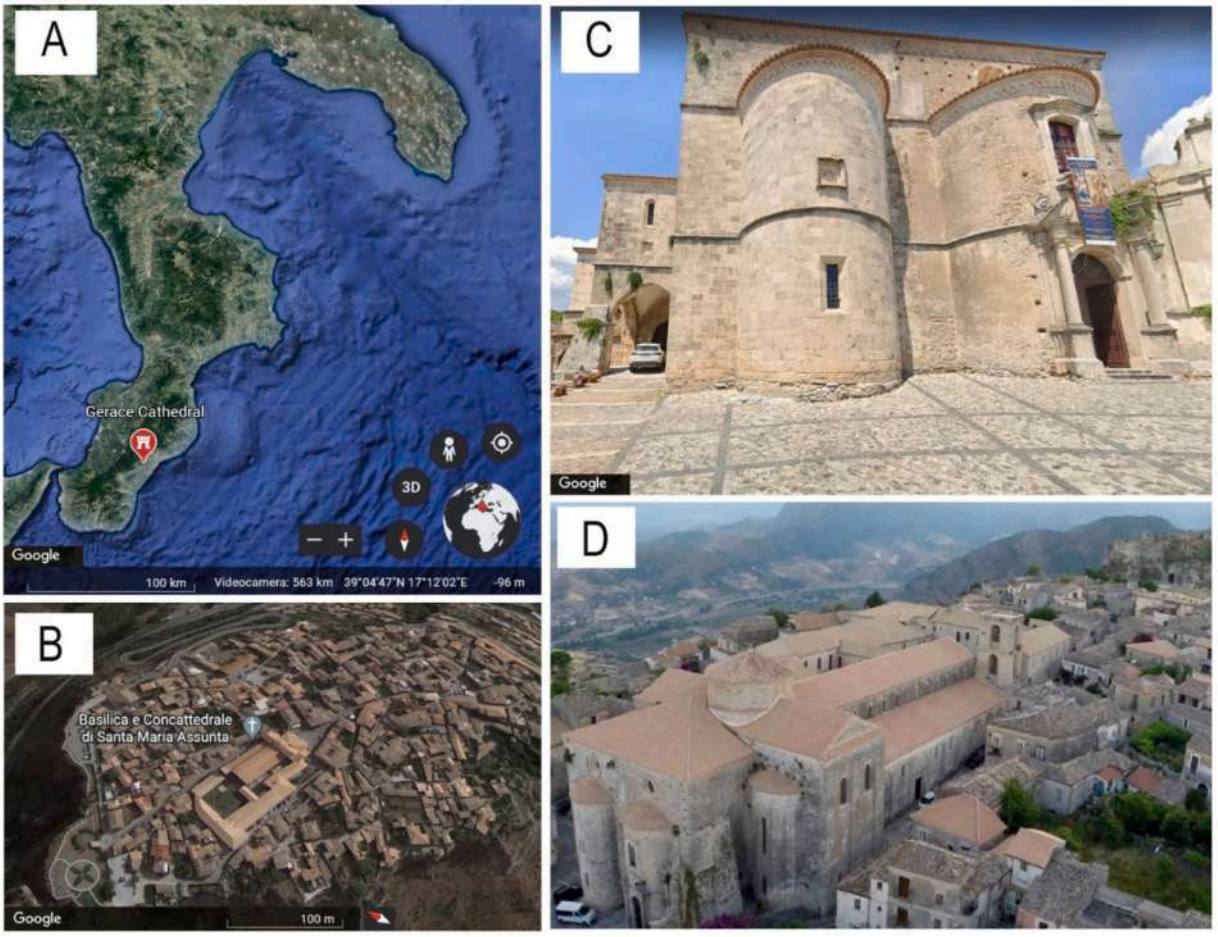

Fig. 1. Location of Gerace in the Calabria region (Italy) (A) and aerial view of the Cathedral within the town (B); Front (C) and panoramic (D) views of the monument. Note: the images were obtained from Google Earth and calabriatours.org.

Calabria in 1659 [10] or the Calabrian seismic sequence of 1783 [11], the building underwent various modifications and renovations over the centuries, while retaining its original structure, characterized by a simplicity of the longitudinal body in contrast with the complex articulation of the presbytery [7]. The structure is built from local stone, a light beige-grayish limestone, devoid of redundant embellishments and with rigorous shapes closely linked to the esthetic-stylistic traits of the Normans [8]. The complex is visibly divided into two overlapping parts dating back to different periods: the underground Crypt and the upper church (the main basilica), the latter with an transept apse to the east and a main entrance to the west. The facade is not entirely visible from the outside, due to the

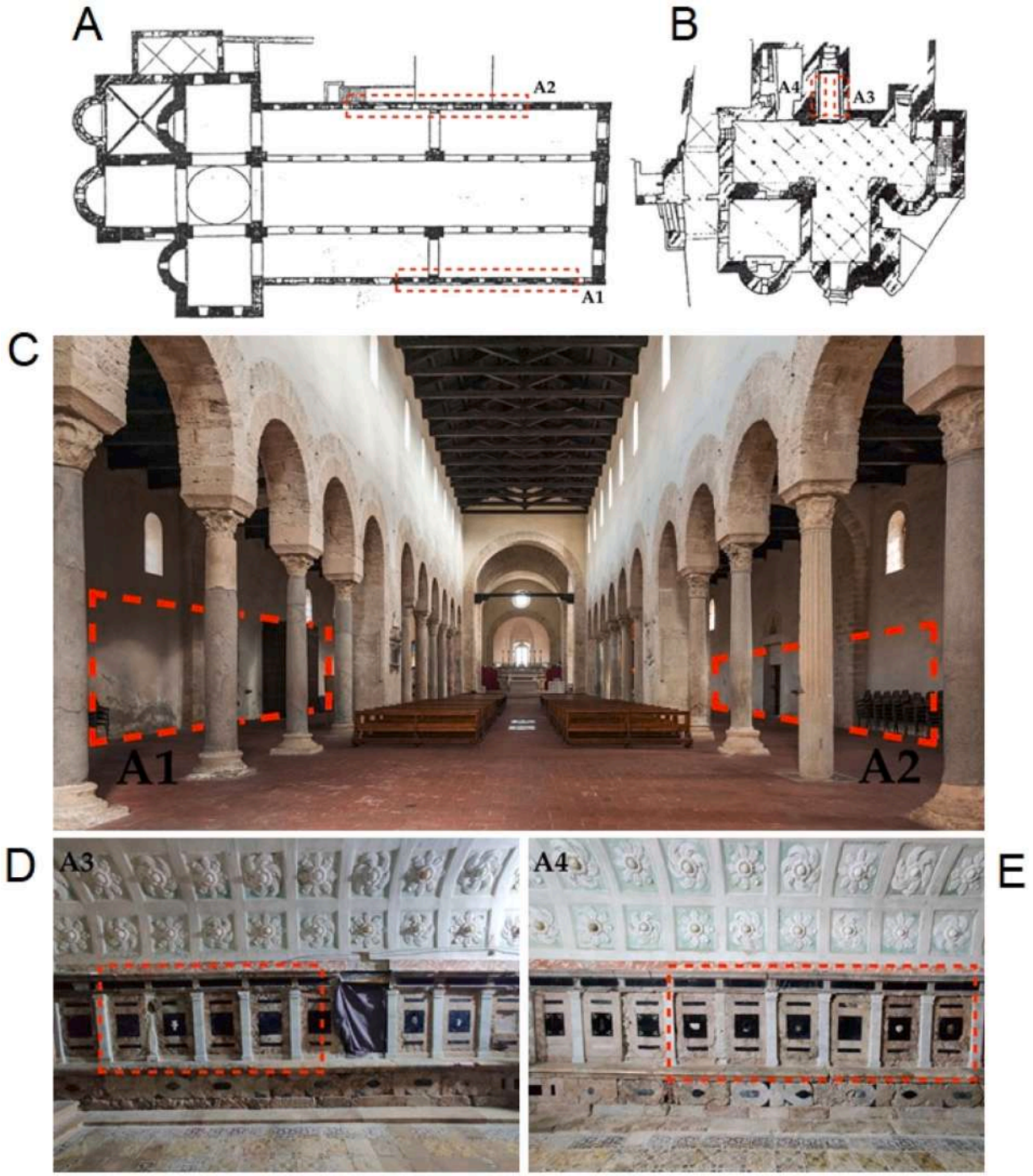

Fig. 2. Plan of the two levels of the Gerace Cathedral: the three-aisled basilica (A), on the upper floor and the Crypt (B), located on the lower floor, with the areas of infrared thermography (IRT) measurements (A1-A4), and some representative images of the sampling areas (C-E). Upper level: (C) left (A1) and right (A2) aisles of the Cathedral; (D-E) the Madonna dell'Itria Chapel: left (A3) and right (A4) walls.

adjacent buildings and especially the bell tower which hides the view of its width [7]. The front is tripartite (with three compartments), Romanesque, and has only very slight pilasters, hanging arches, and elegant splays at the openings [12–14].

The basilica-type church with a large protruding transept has a Latin cross and three naves, separated by two rows of ten columns each in granite and marble, on which stand round arches consisting of local stone and surmounted by as many capitals [7]. The lower part of the Cathedral, the Crypt, can be descended into from the left transept, through seventeenth-century internal stairs [15].

The Crypt is the oldest section of the Cathedral, probably built on a Byzantine rock church [7]. In its current configuration, the Crypt resembles an aggregate of small cross vaults supported by twenty-six slender columns of very different quality and sizes [16]. This area is characterized by a longitudinal arm deriving from a large pre-existing Byzantine oratory, and by a transverse arm, which corresponds to the upper transept of the Cathedral with which it is contemporary [15]. In the Crypt, the Sacello della Madonna dell'Itria, which is carved into the rock, is closed by a seventeenth-century wrought iron gate installed by the workers of Serra S. Bruno [7].

Leaving the Crypt, two of the three semi-circular apses dominate the Piazza della Tribuna and protrude from an imposing limestone wall. These, placed on the same line, are slightly asymmetrical due to seismic events which have been invalidating the structure since the Swabian era [7].

The Cathedral of Maria Assunta of Gerace, despite numerous alterations and restorations, remains the most imposing Norman building in Calabria [17], and has also been declared Architectural Heritage of National Interest. In 1996, following an agreement between the Diocese of Gerace, the Municipality, and the Superintendence, a large intervention was proposed which envisaged, in

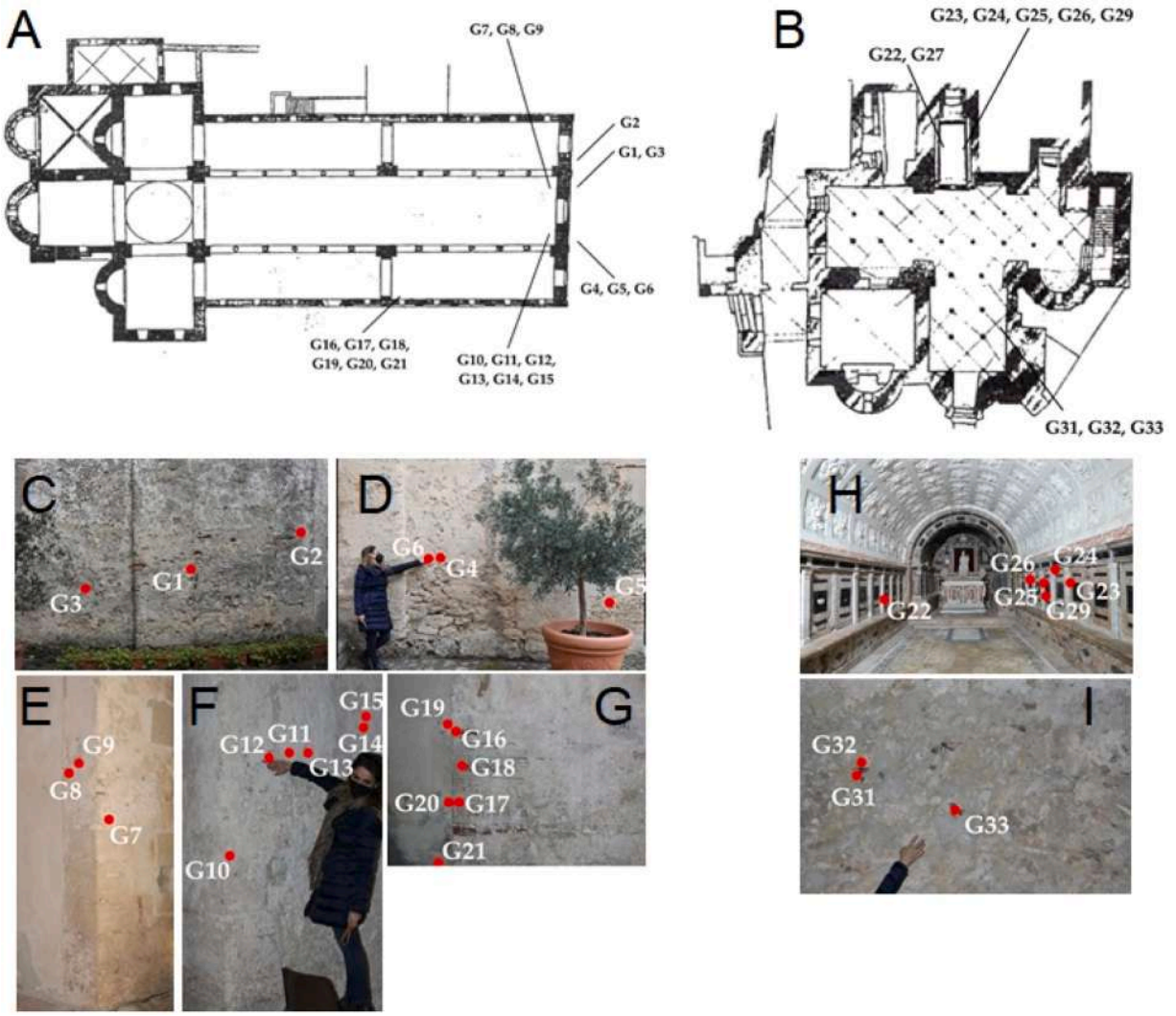

Fig. 3. Plan of the two levels of the Gerace Cathedral: the three-aisled basilica (A), on the upper floor and the Crypt (B), located on the lower floor, with the location of the sampling points, and representative images of the sampling procedure (C-I). Upper level: (C-D) outside the Cathedral's main entrance (G1-G6); (E-F) inside, near the sides of the portal (G7-G15), and (G) on the internal wall of the left aisle (G16-G21). Lower level: (H) inside the Madonna dell'Itria Chapel (G22-G29) and (I) on the internal right wall of the apsidal entrance (G31-G33).

addition to the restoration and consolidation of the structures of the entire extended citadel, its re-functionalization [18].

In recent decades, the structure has displayed areas with a poor state of conservation, which the present study aims to investigate. Specifically, the study was carried out in two phases: a diagnostic stage conducted on-site, and an analytical one, conducted in the laboratory. In particular, the on-site diagnosis phase made it possible allowed us to perform a preliminarily identification and evaluation of the intensity of the degradation forms and to choose the most suitable sampling areas for a more in-depth study. The on-site diagnosis was carried out by means of visual inspections and InfraRed Thermography (IRT). The latter is a non-destructive technique that is widely employed in the analysis of Cultural Heritage [19,20] as it allows the determination of the temperature of a surface by measuring the IR radiation emitted by each object as a function of the temperature, T (°C). This feature has a use in numerous different applications [21]; for example, IRT technique is widely used in building inspection to detect superficial cracks, detachments, different types of materials, or the presence of moisture within structures [22,23]. The temperature distribution on the surface of artefacts, facades, and walls provides very useful information for discovering hidden materials and specific conditions related to their thermal performance, which may also depend on the state of conservation and maintenance interventions [23,24].

Moreover, different kinds of materials (i.e., stones, mortars, plasters and pigments) as well as decay agents (i.e., salt efflorescences) were investigated. The samples were subjected to a complementary analytical approach, specifically involving Polarizing Optical Microscopy (POM), Ion Chromatography (IC), X-Ray Powder Diffraction (XRPD), and Scanning Electron Microscopy coupled with electron-dispersive X-ray spectroscopy (SEM-EDS). The analytical phase allowed us to characterize the stone samples, raw materials, and their degradation forms, and to define the main composition of the pictorial films (i.e., pigmenting compounds/pictorial layers).

2. Analytical methods and sampling

The main purpose of this preliminary diagnostic study was to characterize the main materials and detect any forms of degradation and related causes, in order to provide the necessary information for a future restoration project in areas of the Cathedral suffering from a serious state of deterioration. To this end, the adopted methodological approach involved: a) choosing the study areas of the Cathedral following the requests of experts and restorers in charge of the building maintenance; b) an in situ inspection and evaluation

Table 1
Summary of areas investigated and sampled both with in-situ and laboratory-based methods. POM=Polarizing Optical Microscopy; IC=Ion Chromatography; XRPD=X-Ray Powder Diffraction; SEM-EDS=Scanning Electron Microscopy coupled with electron-dispersive spectroscopy; IRT=InfraRed Thermography.

Area ID	Measurement area	Type	Employed Techniques
A1	Internal wall of cathedral, left aisle	Wall	IRT
A2	Internal wall of cathedral, right aisle	Wall	IRT
A3	Indoor/Madonna dell'Itria Chapel, right side	Wall	IRT
A4	Indoor/Madonna dell'Itria Chapel, left side	Wall	IRT
Sample ID	Sampling area	Type	Employed Techniques
G1	Outdoor/From the main entrance of the basilica	Mortar	POM; SEM-EDS
G2	Outdoor/From the main entrance of the basilica	Mortar	POM; SEM-EDS
G3	Outdoor/From the main entrance of the basilica	Mortar	POM; SEM-EDS
G4	Outdoor/From the main entrance of the basilica	Mortar	POM; SEM-EDS
G5	Outdoor/From the main entrance of the basilica	Stone material	POM
G6	Outdoor/From the main entrance of the basilica	Mortar	POM; SEM-EDS
G7	Indoor/From the portal of the basilica	Plaster	POM; SEM-EDS
G8	Indoor/From the portal of the basilica	Plaster + blackish pictorial film	POM; SEM-EDS
G9	Indoor/From the portal of the basilica	Plaster + blackish pictorial film	POM; SEM-EDS
G10	Indoor/From the portal of the basilica	Plaster + yellowish pictorial film	POM; SEM-EDS
G11	Indoor/From the portal of the basilica	Plaster + blackish pictorial film	POM; SEM-EDS
G12	Indoor/From the portal of the basilica	Plaster + brownish pictorial film	POM; SEM-EDS
G13	Indoor/From the portal of the basilica	Plaster + yellowish pictorial film	POM; SEM-EDS
G14	Indoor/From the portal of the basilica	Plaster + reddish pictorial film	POM; SEM-EDS
G15	Indoor/From the portal of the basilica	Plaster + beige-yellowish pictorial film	POM; SEM-EDS
G16	Indoor/From the left aisle of the basilica	Plaster + reddish pictorial film	POM; SEM-EDS
G17	Indoor/From the left aisle of the basilica	Plaster + green pictorial film	POM; SEM-EDS
G18	Indoor/From the left aisle of the basilica	Plaster + brownish pictorial film	POM; SEM-EDS
G19	Indoor/From the left aisle of the basilica	Salt efflorescences	IC; XRPD
G20	Indoor/From the left aisle of the basilica	Salt efflorescences	IC; XRPD
G21	Indoor/From the left aisle of the basilica	Salt efflorescences	IC; XRPD
G22	Indoor/Madonna dell'Itria Chapel, left wall	Salt efflorescences	IC; XRPD
G23	Indoor/Madonna dell'Itria Chapel, right wall	Salt efflorescences	IC; XRPD
G24	Indoor/Madonna dell'Itria Chapel, right wall	Salt efflorescences	IC; XRPD
G25	Indoor/Madonna dell'Itria Chapel, right wall	Salt efflorescences	IC; XRPD
G26	Indoor/Madonna dell'Itria Chapel, right wall	Stone material	POM
G27	Indoor/Madonna dell'Itria Chapel, right wall	Stone material	POM
G29	Indoor/Madonna dell'Itria Chapel, right wall	Stone material	POM
G31	Indoor/Right wall with respect to Crypt entrance	Plaster + reddish pictorial film	POM; SEM-EDS
G32	Indoor/Right wall with respect to Crypt entrance	Plaster + yellowish pictorial film	POM; SEM-EDS
G33	Indoor/Right wall with respect to Crypt entrance	Plaster + reddish pictorial film	POM; SEM-EDS

of selected areas to be examined; c) an investigation by IRT and micro-destructive techniques following a micro-sampling campaign.

In particular, the inspection of some internal wall surfaces with in-situ methods has proved to be very effective, minimizing contact with already visibly altered surfaces and facilitating the assessment of the state of conservation of the historical building.

For the laboratory investigations, thirty-one samples, including both micro-fragments and powders, were sampled from areas with already existing lacunae and alterations. It is worth underlining that the sampling procedure was conducted according to principles of minimal invasiveness, collecting representative samples. Details on the sampling areas are summarized in Figs. 2 and 3, while all the analytical techniques employed and sampling campaign are described below and further summarized in Table 1.

2.1. InfraRed thermography

In this study, IRT was used to map the surface temperatures, thus revealing the presence of thermal anomalies arising from decay processes affecting the Cathedral as a whole. It is worth noting that particular attention was paid during this phase to investigating the internal walls, in the vicinity of the areas under restoration. The survey was carried out with a FLIR model B335 thermal imaging camera equipped with an uncooled microbolometer (320 ×240-pixel resolution, over a −20 °C to + 120 °C thermal range, +/− 2% of the detected temperature accuracy; 7.5 ÷ 13 μm spectral range; 1.36 mrad spatial resolution; 25° × 19° embraced field). The camera was also equipped with a 3.1 Mpixel photographic sensor that allowed the acquisition of the thermal image at the same time as the visible one, with the same shooting conditions. The images were acquired by positioning the IR camera frontally on the wall surface, a few meters away, in passive mode, thus framing the portion of the wall to be investigated and, at the same time, ensuring a good spatial resolution with a spot size of a few millimeters. The analyzed areas are shown in Fig. 2 and detailed in Table 1.

2.2. Micro-destructive laboratory methods and sampling

Minimal sampling was required for the laboratory-based surveys involving microscopic investigations by POM and SEM-EDS, as well as XRPD and IC. Then, a careful sampling of micro-fragments (sizes smaller than ~5 mm^2) and powders was carried out by selecting areas and collecting different types of representative samples (i.e., stones, plasters, pigments, and salt efflorescences). Minimally invasive procedures were followed for the latter, using suitable stainless-steel tools such as small tweezers, scalpels, and micro-scalpels. The sampling phase was performed on both levels of the building: the upper one, where the Cathedral is located, and lower one, which hosts the Crypt. All of the documentation with the sampling points, together with the type of material and the techniques used, are shown in Fig. 3 and in Table 1.

The Polarized Optical Microscopy (POM) studies of thin stratigraphic sections were conducted in order to characterize the main materials present at the site, including the stones, mortars, and what remains of some ancient wall paintings. Observations were performed on twenty-four samples using a Primotech 40 (Primotech Zeiss) microscope coupled with a digital camera to capture images.

The SEM-EDS analyses allowed us to investigate the samples in greater detail, both from a morphological and compositional point of view. Chemically (in terms of major elements), the method helped investigate not only the properties of the materials but also their associated alteration products [25]. Investigations were carried out on samples coated with a thin and highly conductive graphite film using an ultra-high resolution SEM (ZEISS CrossBeam 350 equipment), coupled with a EDS – EDAX OCTANE Elite Plus - Silicon drift type detector. type.

X-Ray Powder Diffraction (XRPD) is commonly used in materials science to determine the crystallographic structure of crystalline solids [26]. In this study, XRPD was specifically used to determine the mineralogical phases constituting the samples of salt efflorescences [27]. The analyses were performed with a Bruker D8 Advance X-Ray diffractometer (Bruker, Karlsruhe, Germany), with Bragg-Brentano geometry and a copper sealed tube X-ray source producing Cu kα radiation (wavelength of 1.5406 Å) from a generator operating at 40 kV and 40 mA. The diffracted X-rays were recorded on a scintillation counter detector located behind a set of long Soller slits/parallel foils. Scans were collected in the range of 3–65° 2θ, using a step size of 0.014° 2θ and a step counting time of 0.2 s. The EVA software (DIFFRACplus EVA version 11.0. rev. 0) was used to identify mineral phases by comparing experimental patterns with 2005 PDF2 reference patterns.

Ion Chromatography (IC) can be used to determine ion concentrations in an unknown sample [28]. In Cultural Heritage studies, as in this study, it has been used to identify the nature of the soluble salts and to quantify them [29]. A Dionex DX 120 equipment on a filtered supernatant (filter Minisart RC 25, diameter = 0.45 μm) provided the IC data, with the determination of the following ionic species: PO_4^{3-}, SO_4^{2-}, NO_3^-, Cl^-, F^-, Br^-, Li^+, $NH4^+$, Na^+, K^+, Ca^{2+}, Sr^{2+} and Mg^{2+}. The determination of HCO_3^- was carried out by acid-base titration with HCl.

3. Results and discussion

3.1. InfraRed thermography

The IRT mapping of the surface thermal distribution supported the evaluation of the conservation state of the masonry [30,31], especially where damage forms were macroscopically considerable.

The measurements carried out on the upper floor of the Cathedral, allowed a more accurate determination of the extent of the visible detachments between the layer of plaster and the underlying masonry. The thermographs revealed the presence of thermal discontinuities on both the left (frame A1 in Fig. 4) and right aisles (frame A2 in Fig. 4) of the Cathedral. These discontinuities are

mainly located in the lower part of the masonry (up to a height of ~ 1.5 m), where manifestations of damage (i.e., loss of surface material and white salt efflorescences) were also visible to the naked eye. The IRT images also highlighted superficial swellings and micro-cracks in the plaster, suggesting the presence of moisture in the walls and most likely the formation of sub-efflorescence. Rising damp is generally related to water infiltration and migration phenomena that seem to affect a significant part of the building. The crystallization of salts below the material surface (sub-efflorescence) will generally occur when the evaporation rate is greater than the migration rate of a solution towards the exterior of a material. The inverse process instead determines the formation of external efflorescence caused by the crystallization of deposited salts [32]. In more detail, the IR images of the investigated areas (frames A1 and A2 in Fig. 4) show that efflorescence phenomena can be detected by IRT; in fact, a correspondence can be observed between the areas with white salt efflorescence and surface temperature anomalies with respect to the surrounding masonry portions. Cooler temperatures (from cyan to dark blue on the colors scale i.e., less heat and infrared radiation emitted) are found in the lower part of the masonry (up to ~30 cm in height), as shown by the vertical temperature profiles in the figure, which is certainly more exposed to environmental cooling as well as being subject to capillary rising phenomena and efflorescence. Otherwise, warmer sectors (from orange to red on the color scale, i.e., emitting more heat and infrared radiation) are found where the masonry shows a lower degree of weathering, namely in those portion of the wall that are not affected by efflorescence but by micro-cracking, flaking, and detaching phenomena (at a height between 30 cm and 1.50 m).

Thermographs of the Crypt, whose walls are covered with slabs of stone materials of various kinds, allowed us to carry out the first mapping of the presence of moisture in the masonry and to relate it to the possible presence of dissolved salts that could cause alteration phenomena. In many cases, the ornamental slabs showed an evident detachment from the wall, probably as a result of mechanical stress due to the presence of moisture and the consequent formation of salts especially as sub-efflorescences. For example,

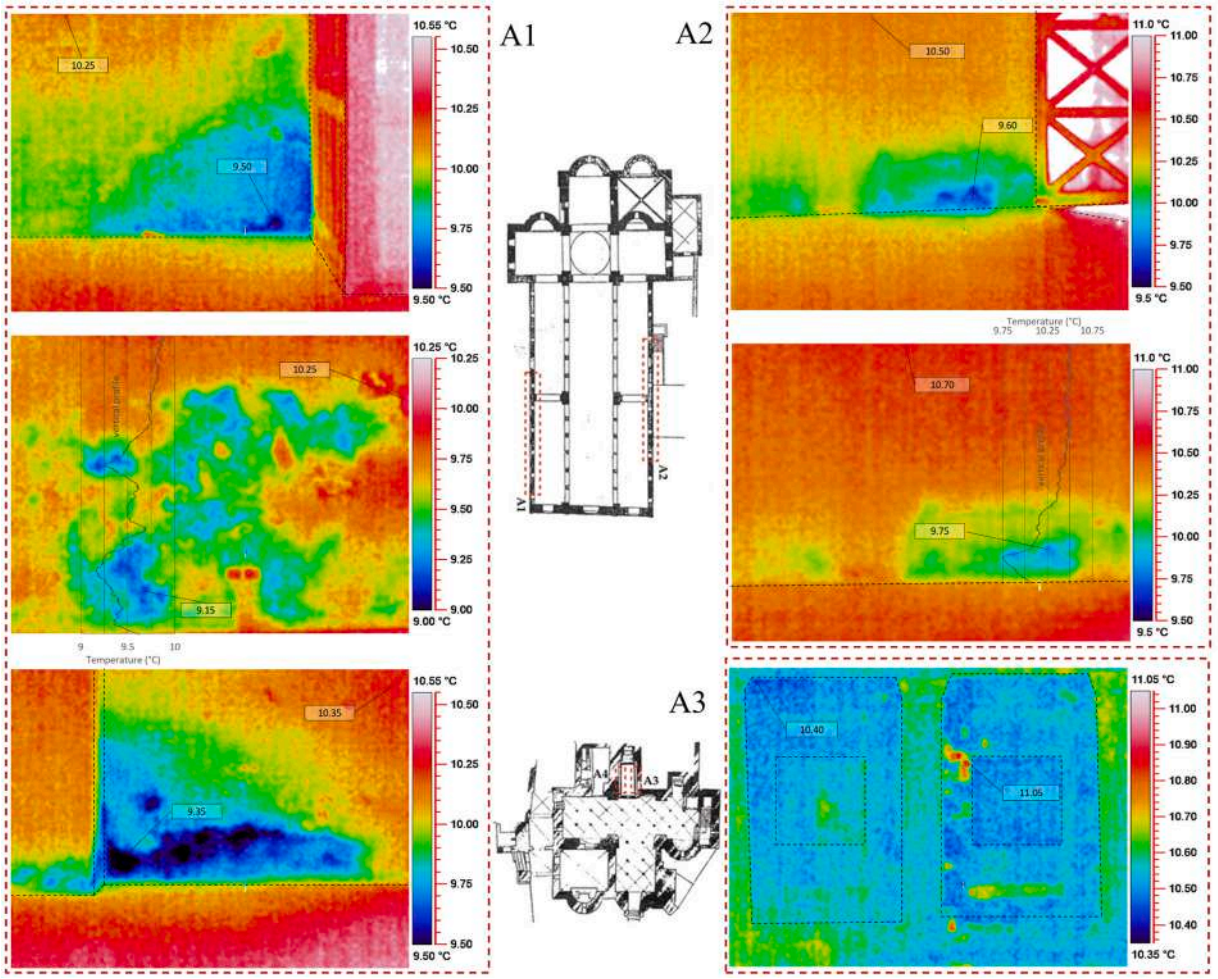

Fig. 4. Representative infrared thermography (IRT) images of the investigated areas. Upper level: left (Zone A1) and right (Zone A2) aisles of the Cathedral. Lower level: right wall inside the Madonna dell'Itria Chapel (A3). The highest and lowest temperatures are reported in the boxes for all IRT images. The vertical temperature profiles are sketched both for the right and left aisles (gray lines). In addition, the edges of the walls and other decorative elements are delineated with thin black dashed lines for a better understanding. Note: Visible images of investigated areas by IRT are shown in Fig. 2.

the thermal image related to the right wall of the Crypt (frame A3 in Fig. 4) shows evident cracks near the hotter areas (reddish-yellow tones on the color scale and a temperature around 0.25 °C greater than in the cooler areas) indicating an advanced degradation of the covering materials up to detachments in small parts.

3.2. Micro-destructive laboratory methods

Thin section of 24 micro-fragments were manufactured for petrographic analysis. Observation under POM allowed us to identify the main minero-petrographic and textural features of the stones, mortars, and plasters with pictorial films, as well as evaluating their state of conservation. The petrographic results are described for each of the samples, highlighting their main features, which serve to link or separate them from each other; in fact, where they are similar, the samples are described as a single group. Some representative photomicrographs are shown in Fig. 5, while Table S1 reports the main petrographic features detected for each sample.

3.2.1. Group 1 - samples G5, G26, G27, & G28: stone materials (Type S)

This group includes different kinds of stone materials (i.e., rock) present in the historic building, taken both from the Crypt and from the upper basilica (Fig. 5H, GI; Table S1). Specifically, sample G5, which was obtained from an external area near the portal of the basilica, represents the constituent material with which the Cathedral is built. It is a bioclastic calcarenite containing abundant bioclasts as well as single crystalline inclusions, and rock fragments. Specifically, quartz crystals, micas (both biotite and muscovite), and oxides were identified together with fragments of metamorphic rocks, carbonate lithoclasts, and rare granitoids. All grains are bound together by a fine-grained calcite (micrite). The porosity is both primary and secondary (15%), with evident fillings by secondary

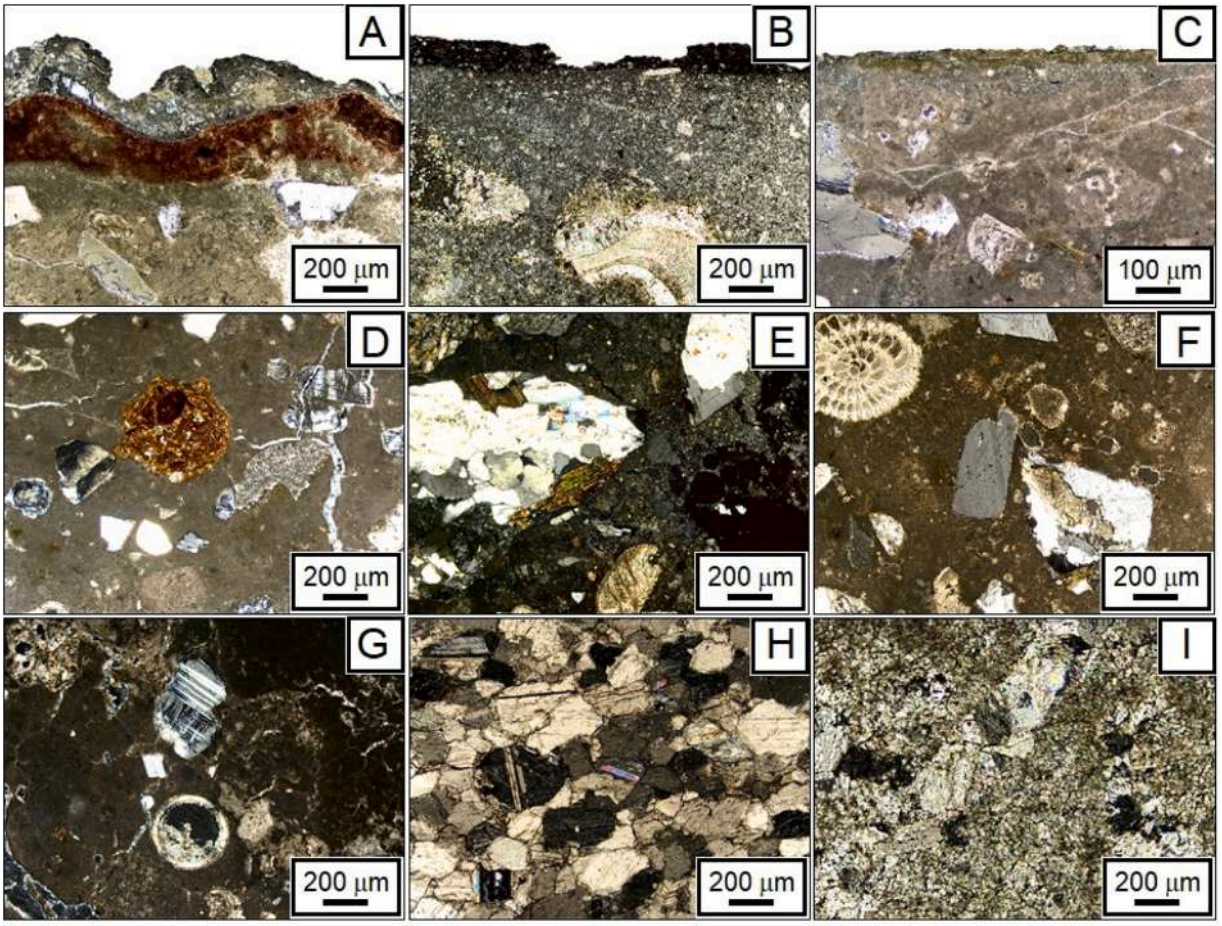

Fig. 5. Representative cross-polarized light (CPL) photomicrographs of the studied samples; G31 (A) – Group 3/Type P/PF: sample stratigraphy with evidence of the three layers, i.e., plaster, reddish pictorial film and the scialbo; G12 (B) - Group 3/Type P/PF: sample stratigraphy with evidence of two layers, i.e., plaster and the brownish pictorial film; G32 (C, F) - Group 3/Type P/PF: sample stratigraphy with evidence of two layers, i.e., plaster and the yellowish pictorial film; G4 (D) - Group 2/Type M: detail of the mortar samples with quartz crystals, cocciopesto, and rock fragments; G7 (E) - Group 3/Type P/PF: detail of the plaster layers with quartz crystals and granitoid rock fragments; G6 (G) - Group 2/Type M: detail of the mortar samples with quartz crystals, granitoid rock fragments, and bioclasts; G29 (H) - Group 1/Type S: fine grained "mosaic" type marble; G27 (I) - Group 1/Type S: microcrystalline limestones calcite veins.

recrystallized calcite. Accordingly, the stone sample can be classified as a biocalcarenite or packstone [33,34]. The data are also consistent with the literature [35,36], according to which this kind of stone is widely used in the Gerace area as a constituent material of the large-scale built cultural heritage. Samples G26 and G27, obtained from the ornamental slabs that cover part of the Crypt's walls, are microcrystalline limestones which host calcite veins made up of well-formed crystals. The samples are in an advanced state of alteration with evident microfractures and secondary porosity. Finally, sample G29, s from a covering slab of the Crypt, is a marble characterized by a fine grain size (MGS <1 mm;) and a generally homeoblastic (Ho) texture. The fabric is commonly of "mosaic" type, with small to very small crystals, which in some places form triple point junctions (120°). Slightly lineated or weakly oriented fabrics were also observed. The grain size ranges from 0.1 mm to 0.9 mm, often with clear traces of cleavage, while the grain boundary shape (GBS) varies from curved to straight. A shape preferred orientation (SPO) of the grains was not observed nor were accessory minerals.

3.2.2. Group 2 - samples G1, G2, G3, G4, & G6: Mortars (Type M)

All the samples belonging to Group 2, were taken from the external facade of the building, at the entrance to the upper basilica (Figs. 5D, 5G; Table S1). They are mortars characterized by a brownish micritic binder in Crossed Polarized Light (CPL), in which the aggregate fraction varies from well-sorted to moderately and poorly selected, and mainly consists of mono- and polycrystalline quartz crystals, micas, calcite, and various bioclasts. Like other inclusions, feldspars, oxides, and rare pyroxenes are present to a lesser extent. Fragments of volcanic (granitoids), metamorphic, and carbonate rocks were also detected. All samples, except for G4 and G6, contain a layer of finishing mortar (layer B) with the same mineralogical composition as the main layer (layer A) but with a finer grain size. Samples G1, G2, and G4 also host sporadic cocciopesto inclusions. In terms of size, individual mineralogical phases vary from 400 μm to 1500 μm, while rock fragments reach dimensions of up to 2800 μm, with angular to sub-angular and to rounded to sub-rounded shapes. Fractured lumps with defined edges were also detected in all the samples, having a sub-spherical shape with diameters ranging from 400 μm to 2000 μm. The presence of a finishing layer in samples G1, G2, and G3 could be related to a previous restoration procedure which was probably carried out to consolidate the limestone ashlars. Unfortunately, there is no documentation of past restoration interventions in the archives, but oral sources suggest various interventions to the building over time.

3.2.3. Group 3 - samples G7, G8, G9, G10, G11, G12, G13, G14, G15, G16, G17, G18, G31, G32, & G33

Plasters with pictorial films (Type P/PF). The samples belonging to this group consist of plasters (layer A), covered with a very thin layer of pictorial film (layer B – up to 260 μm) (Figs. 5A, 5B, 5C, GF; Table S1). Some specimens contain a finishing layer, probably a "scialbatura" (layer C - up to 350 μm) (samples G8, G10, G11, G14 and G31). More specifically, the term "scialbatura" or "scialbo" refers to a layer of light, fine, and thin plaster covering a mural painting. From a mineralogical point of view, layer A consists of a plaster containing a fairly homogeneous micritic binder (sometimes cryptocrystalline) in which the aggregate fraction varies from well-sorted to moderately and poorly selected. The coarse fraction is mostly constituted by monocrystalline quartz granules and polycrystalline ones, followed by micas, calcite, bioclasts, iron oxides, and rare feldspars, with sizes reaching 1400 μm and shapes varying from angular to sub-angular and to rounded to sub-rounded. Fragments of rocks (volcanic, metamorphic, and calcareous) and rare cocciopesto with sizes reaching 4050 μm were also detected. The percentage of the aggregates in layer A varies from 20% to around 50% (by area) [37]. The latter was assessed by means of a semi-quantitative visual estimation. The porosity of the same layer A varies from about 5–15% (by area) and it consists of both primary and secondary pores with sizes of up to 700 μm. In addition, recrystallization phenomena of the calcite were observed in the voids. The pictorial layer (layer B) appears to be very thin, sometimes with sporadic crystals of calcite occurring together with oxides. The color of the different samples appears to be reddish to brownish and yellowish under Plane Polarized Light (PPL). Finally, layer C, where present consists of microcrystalline calcite, with thicknesses of up to 350 μm.

The SEM-EDS analyses were performed on thin and stratigraphic sections of the samples belonging to Group 2 (Type M) and Group 3 (Type P/PF) (Fig. 5, Table S1). The binder's composition in the different layers, the raw materials, and the stratigraphy were investigated, paying special attention to the pigmented layers and the overlying ones (scialbo), where present.

For the Group 2 samples (G1-G4, G6) and those consisting of mortars, the morphological observations by SEM confirmed the OM data, highlighting the presence of two overlapping mortar layers for all the samples, except for G4 and G6. Five EDS measurements were performed on the binders of each layer present in the samples, and the average values were considered as representative of their chemical compositions (since no significant variations were observed when calculating the standard deviation relative to the mean values of the EDS dataset). Regarding the major elements, a large amount of CaO was detected in all the samples, in addition to significant SiO_2 and MgO concentrations, followed by lower amount of $Al2O_3$ and Na_2O. The presence of Mg suggests that the lime was likely formed through the calcination of magnesian limestone and/or dolostone. This latter assumption was further confirmed by the EDS measurements performed on lumps (three spot analyses in their central portion to reduce contamination), suggesting the use of magnesian lime-based mortars. Furthermore, considerable amounts of Sr and SO_4 were also present, which may have been related to the use of evaporites as raw materials. In fact, celestine minerals (sulfates) were also found sporadically in the aggregate fraction and these may have precipitated as euhedral crystals after the liberation of Sr [38–40]. This could also indicate that the original raw materials were sourced from Gerace area [35,36].

The morphological investigations of the samples belonging to Group 3 further with the OM data. Furthermore, the study of the binders conducted on the layers of plaster (layers A) revealed a chemical composition similar to that of the mortars of Group 2, confirming the use of the same raw materials for the plastering production. Specifically, our results suggested the presence of a magnesian lime-based plaster in all the samples, resulting from the calcination of Mg-limestones. In layer B, elements such as Si, Al, Mg, and K were mainly detected in blackish, brownish, green, and beige-yellowish pictorial films (samples G8, G9, G10, G11, G12, G13, G15, G17, G18). In addition, Fe was also detected in the beige-yellowish pictorial layers (G10, G13, G15, G32). Such elements are compatible to the possible use of raw materials from clay and other minerals that are commonly found in soils and were likely used as

pigmenting compounds [41–47]. The EDS analyses of the reddish layers (samples G14, G16, G31, G33) highlighted mainly the presence of Hg and S (Fig. 6-G31_c) along with elements attributable to earthy pigments, suggesting the use of a mixture of cinnabar or vermillion [30] with oxide and/or clay-based pigments; in fact, morphologically, the reddish pigmenting agents are heterogeneously distributed within the layers (Fig. 6; G31_b). Finally, the C layers (scialbo), where present, always consisted of $SrSO_4$ and CaO for all analyzed samples (Fig. 6; G8_b and G8_c).

The IC analyses allowed us to investigate the ionic species contributing to the damage within the walls. In general, the damage caused by soluble salts in building materials can be produced as a result of several mechanisms based on the kind of crystallization taking place [48]. The soluble fraction of major anions for all the analyzed samples mainly consisted of sulfate (SO_4^{2-}) and hydrogen carbonate (HCO_3^-), as well as lesser amounts of nitrate ions (NO_3^-) and chloride (Cl^-); among the cations, Na^+ and Ca^{2+} were the most abound in all samples, followed by less abundant K^+ and Mg^{2+}, along with traces of Sr^{2+}.

A preliminary analysis of the data (Fig. 7) suggested that sulfates and carbonates were the main soluble species present in the investigated areas followed by nitrates and chlorides. For the sulfates, the overall data suggested the presence of sodium sulfates, as well as lower amounts of calcium and magnesium sulfates. Significant differences between the soluble species detected in the samples of the main Cathedral (G19–21) and those of the Crypt (G22–25) should be underlined. Specifically, the samples from the Crypt contained low concentrations of alkaline ions (i.e., Na^+, K^+), possibly due to the greater humidity that generally prevails in an underground environment; such conditions can inhibit the precipitation of sodium/potassium salts, since the latter are generally more soluble than calcium/magnesium salts [49]. Considering the scarcity evidence of sodium ions and the low magnesium ion contents, gypsum may have crystallized as one of the main salts in the Crypt samples, but not the only one. Indeed, gypsum may form if the

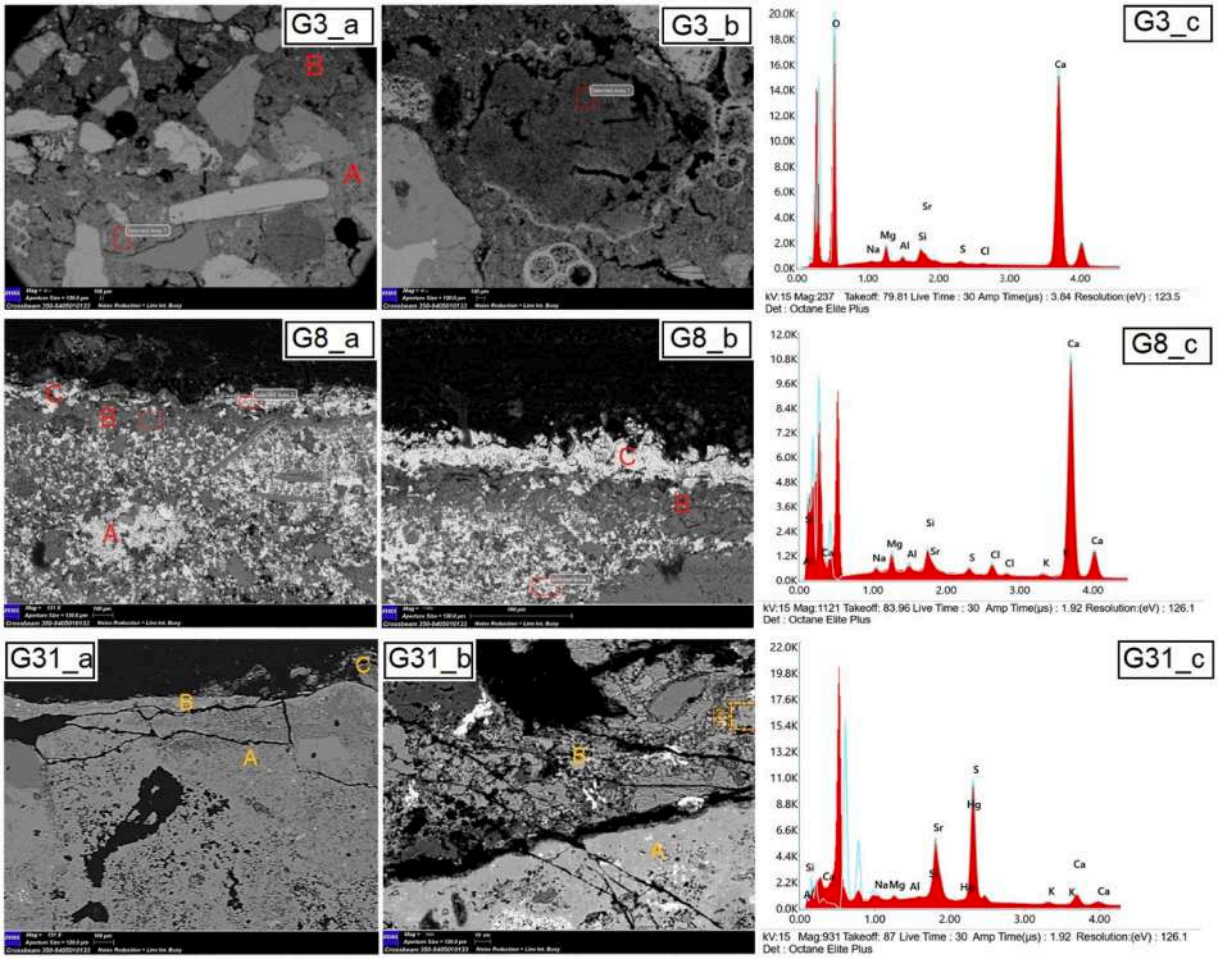

Fig. 6. Representative scanning electron microscopy (SEM) images of thin sections showing the stratigraphy and details of the studied samples; G3_a) sample G3 with evidence of two layers named (A) and (B); G3_b) sample G3 with evidence a fractured lump with defined edges; G3_c) electron-dispersive spectroscopy (EDS) spectrum of sample G3 detected in the binder of layer A; G8_a) sample G8 with evidence of three layers named (A-plaster), (B-pictorial film), and (C-scialbo); G8_b) sample G8 with clear evidence of the two most superficial layers (B and C); G8_c) EDS spectrum of sample G8 detected in layer C (scialbo) where the brightest features represent celestine crystals ($SrSO_4$); G31_a) sample G31 with evidence of three layers named (A-plaster), (B-pictorial film), and (C-scialbo); G31_b) sample G31 with clear evidence of layers named (A) and (B); G31_c) EDS spectrum of sample G31 detected in the pigmented layer B (reddish layers) showing a poor distribution of pigmenting agents.

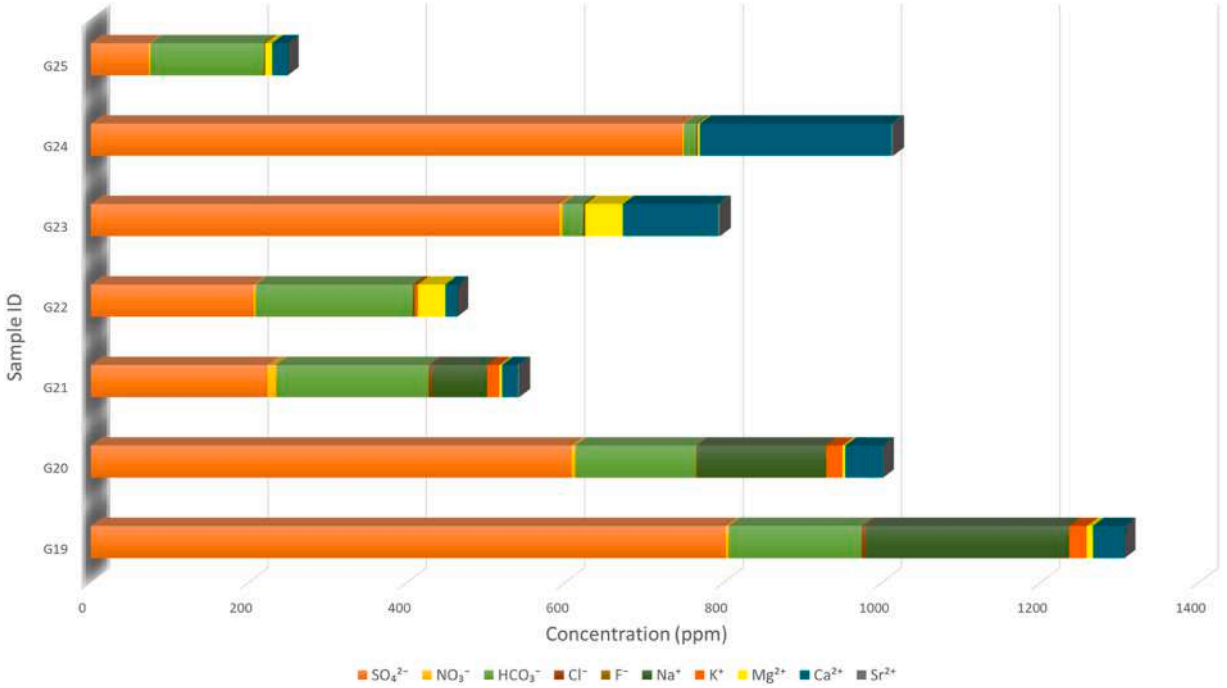

Fig. 7. Concentrations of ionic species expressed in ppm.

relative humidity of an environment becomes lower than the relative humidity at equilibrium (RHeq) of the saturated salt solution in the system [50]. In fact, among the recognized salts, the gypsum has the highest deliquescence RH, which is around 99.6% at 20 °C [51], implying that such a phase is stable even under extremely humid conditions [41].

However, the calcium sulfate (gypsum) could have different origins; for example, it can derive from the original materials (i.e., building materials, rocks, raw materials) or have a different source altogether (i.e., environment). Both options were feasible in this study. The gypsum may have originated from the plaster covering the wall surfaces or from the soil surrounding the building; in the latter case, the sulfate species may have been dissolved in soil water and may have crystallized on the wall surfaces through capillary action.

For the carbonates, Ca was the second most abundant cation in the samples, which could be partly attributed to the intrinsic composition of the investigated materials and/or to their long-term coexistence with lime-rich materials (e.g., plasters, lime mortars) under moist conditions.

In addition, the presence of magnesium sulfate could not be excluded for the Crypt samples G22 and G23. For the latter two, values between 34 and 48 ppm were detected against a threshold of less than 9 ppm detected for all other samples.

When evaluating the contribution of the other soluble species detected by IC, the presence of nitrates in all the samples analyzed, albeit in minimal concentrations, should also be noted. Nitrates, such as potassium and calcium nitrate, can originate from soils through microbiological activity decomposing organic nitrogenous products. The presence of nitrates in masonry, as well as for the other salts, is in accordance with the rising damp phenomena described by Arnold and Zehnder [49] in a scheme showing the vertical fractionation of soluble salt species on a wall; the most soluble and hygroscopic salts (e.g., magnesium and calcium nitrates) reached higher heights on the surface of the wall than less soluble and less hygroscopic salts (e.g., sulfates) which accumulated in the lower portions of the masonry. Even chlorides, like nitrates, are highly soluble and may cause serious damage in the presence of high moisture contents within masonry due to their hygroscopicity. This may lead to decay phenomena that generally occur in masonry with high and permanent moisture contents. The IC results are summarized in Fig. 7.

The XRPD analysis of the efflorescence samples (G19-G25) revealed that calcite was the dominant phase in all the samples from the Crypt, except for G23 and G24. Among other more abundant crystalline phases, the following were detected: thenardite (sodium sulfate) only in the Cathedral samples (G19-G21); gypsum (calcium sulfate) in all samples except in G19 (from the Cathedral) and hexahydrite (magnesium sulfate hexahydrate) in all samples of the Crypt except in G24. Non-soluble minerals such as quartz, clay minerals, magnesite, hydromagnesite, and feldspars were also identified in low concentrations. The data support the IC investigation suggesting that sulfates and carbonates are the most abundant soluble phases.

As for the sulfates, thenardite was exclusively present in the samples of the main Cathedral while hexahydrite and gypsum occurred in those from the Crypt. Traces of gypsum were also found in the Cathedral samples, namely G20 and G21. The origin of these salts could be linked to the interaction (weathering) between capillary rise water and the stone/plaster substrates. Elements such as Mg^{++}, Na^{+}, SO_4^{2-} and Ca^{++} are preferentially leached from substrates, recombining under specific microclimatic conditions in the efflorescences salts following their mobilization through the pore network of the substrates. The presence of calcite has resulted from the

carbonate substrate or to the lime-based plaster covering the building's surface, while the quartz, clay minerals, and feldspars could have been related to the composition of the mortar/plaster (sandy aggregates). Sulfate salts act as rock-decaying agents which may lead to a poor state of cultural heritage conservation. As is well known, one of the major causes of rock decay in nature [52] and weathering of natural and/or artificial building material [53–55] is the presence and crystallization of these soluble salts from repeated cycles of crystallization/dissolution within the matrix of porous stone materials. Furthermore, differences in the semi-quantitative estimates of the mineral phases recognized in the two sampled areas may depend on various factors such as differences in sampling heights on the masonry, the interaction of the samples with adjacent materials of diverse nature, environmental conditions, as well as different levels of mobility and the migration of salts through the masonry [49]. The results of the XRPD analyses are summarized in Table 2.

4. Conclusions

A multidisciplinary approach employing non-destructive and micro-destructive methods was adopted to assess the state of conservation of the Gerace Cathedral. The results showed that:

1. The IRT method is a useful non-contact tool that could be applied for a rapid preliminary evaluation of the weathering state of the building. The technique allowed a preliminary zonation and mapping of the weathering processes affecting the Cathedral's masonry. Such non-destructive methodologies are particularly relevant when studies must be conducted rapidly, especially for preliminary assessments or monitoring purposes when imminent restoration work is expected. It is worth underlining that the reported data herein refer to preliminary surveys and further studies should be performed to investigate the thermo-hygrometric conditions of the historical building.
2. The IC and XRPD analyses of salt efflorescence samples helped confirm that salts contribute to the deterioration of the stones, walls, and mural paintings of the Cathedral, resulting in weathering products of cultural heritage materials. Specifically, salt accumulations in walls mainly originated from the ions leached from rocks, soils, stone, and other raw materials used in the building. Overall, the application of the IC analytical procedure allowed us to quantify the amounts of major cations and anions. The analytical data suggested that sulfates and carbonates are the most abundant soluble species present in the two investigated areas, followed by nitrates and chlorides. Furthermore, the concentrations of the different species were notably different between the two sampled environments, i.e., the Crypt and the upper basilica. These differences were closely related to the environmental conditions, such as the higher humidity of the underground environment. The mineralogical studies by XRPD were in full agreement with the IC results.
3. Microscopic observations by OM allowed us to distinguish different layers among samples and especially those with a pictorial film. In general, in all samples contained similar raw materials, especially those belonging to Groups 2 and 3, confirming a local origin. The presence of a finishing layer of mortar found only in some samples from Group 2 also suggested that an undocumented restoration intervention probably took place in the past. The rock samples (Group 1), on the other hand, were characterized as marbles and crystalline limestones. In the latter case, it was impossible to establish their provenance and further studies will thus be conducted on these materials of unknown origin.
4. The SEM-EDS investigations revealed the presence of similar elements/compounds for all the examined samples, attesting to the use of Mg-lime-based plasters/mortars and lime derived from the calcination of carbonates of evaporitic origin. The layers of scialbo exhibited the same composition, and this material probably derived from previous undocumented restoration interventions. In the painted layers, on the other hand, inorganic chromophores based on natural mineral pigments were found to produce blackish, brownish, green, and yellow shades of color. The use of cinnabar or vermilion, mixed with earthy pigments, was confirmed for the reddish layers.

Finally, this work allowed us to characterize and preliminarily evaluate the state of conservation of the Gerace Cathedral building materials, providing useful data for the planning of future restoration interventions. In fact, in the context of scientific research conducted on Cultural Heritage, the approach represents a necessary prerequisite for planning the best restoration and protection plan possible. A holistic and integrated approach should always be followed for the preservation of cultural heritage, prior to any restoration interventions. Further studies will be conducted to acquire a better understanding of other pilot areas within the Cathedral suffering from a poor state of conservation.

Declaration of Competing Interest

The authors declare that they have no known competing financial interests or personal relationships that could have appeared to influence the work reported in this paper.

Data availability

Data will be made available on request.

Table 2
Minerals occurring in the analyzed samples.

Samples	Thn	Cal	Qtz	Hhy	CM	Gy	Hmgs	Mgs	Fs
G19	xxx	xx	x	-	r	-	-	-	-
G20	xxx	xx/x	r	-	r	x	r	r	-
G21	xxx/xx	xxx	r	-	r	r	-	-	r
G22	-	xxx	-	xx/x	x	-	-	-	-
G23	-	-	-	xxx/xx	-	xxx	-	-	-
G24	-	-	-	-	-	xxx	-	-	-
G25	-	xxx	-	r	-	x	-	-	-

Notes: Thn=Thenardite; Cal = Calcite; Qtz = Quartz; Hhy = Hexahydrite; CM = Clay Minerals; Gy = Gypsum; Hmgs = Hydromagnesite; Mgs = Magnesite; Fs = Feldspars; xxx = abundant; xx = moderate; x = poor; r = rare.

Appendix A. Supporting information

Supplementary data associated with this article can be found in the online version at doi:10.1016/j.cscm.2023.e02225.

References

[1] E.T. Delegou, G. Mourgi, E. Tsilimantou, C. Ioannidis, A. Moropoulou, A multidisciplinary approach for historic buildings diagnosis: the case study of the Kaisariani Monastery, Heritage 2 (2019) 1211–1232, https://doi.org/10.3390/heritage2020079.
[2] A. Moropoulou, K.C. Labropoulos, E.T. Delegou, M. Karoglou, A. Bakolas, Non-destructive techniques as a tool for the protection of built cultural heritage, Constr. Build. Mater. Volume 48 (2013) 1222–1239, https://doi.org/10.1016/j.conbuildmat.2013.03.044.
[3] F. Sandrolini, E. Franzoni, G. Cuppini, L. Caggiati, Materials decay and environmental attack in the Pio Palace at Carpi: a holistic approach for historical architectural surfaces conservation, Build. Environ. Volume 42 (Issue 5) (2007) 1966–1974, https://doi.org/10.1016/j.buildenv.2006.04.021.
[5] (a) F. Sandrolini, E. Franzoni, E. Sassoni, P.P. Diotallevi, The contribution of urban-scale environmental monitoring to materials diagnostics: a study on the Cathedral of Modena (Italy), J. Cult. Herit. Volume 12 (Issue 4) (2011) 441–450, https://doi.org/10.1016/j.culher.2011.04.005;
(b) L. Berto, A. Doria, P. Faccio, A. Saetta, D. Talledo, Vulnerability analysis of built cultural heritage: a multidisciplinary approach for studying the Palladio's Tempietto Barbaro, Int. J. Archit. Herit. 11 (6) (2017) 773–790, https://doi.org/10.1080/15583058.2017.1290853.
[6] E. Spoldi, I. Ippolito, A. Stella, S. Russo, Non-destructive techniques for structural characterization of cultural heritage: a pilot case study, Struct. Control Health Monit. 28 (2021) 12, https://doi.org/10.1002/stc.2820.
[7] V. Cataldo, Gerace La Cattedrale, Nosside, 2001.
[8] G. Occhiato Le Chiese dell'età normanna alle forme rinascimentali I Beni Cult. e Le. chiese di Calabr., Laruffa, Reggio Calabr. 1981 346.
[9] C. Bozzoni, L'organismo architettonico, in: S. Gemelli, C. Bozzoni, La Cattedrale di Gerace, Cassa di risparmio di Calabria e Lucania, Effesette, Cosenza, 1986, pp. 84–99.
[10] E. Guidoboni, G. Ferrari, G. Tarabusi, G. Sgattoni, A. Comastri, D. Mariotti, C. Ciuccarelli, M.G. Bianchi, G. Valensise, CFTI5Med, the new release of the catalogue of strong earthquakes in Italy and in the Mediterranean area, Sci. Data 6 (80) (2019) 2019, https://doi.org/10.1038/s41597-019-0091-9. ⟨https://doi.org/10.1038/s41597-019-0091-9⟩.
[11] A. Costanzo, A. D'Onofrio, F. Silvestri, Seismic response of a geological, historical and architectural site: the Gerace cliff (southern Italy), Bull. Eng. Geol. Environ. 78 (2019) 5617–5633, https://doi.org/10.1007/s10064-019-01515-0.
[12] C. Bozzoni, Calabria Normanna, Ricerche sull'architettura dei secoli undicesimo e dodicesimo, Off. Roma (1974).
[13] P. Pensabene, Marmi di rimpiego, in: La Cattedrale di Gerace, Cassa di risparmio di Calabria e Lucania, Effesette, Cosenza, 1986, pp. 127–143.
[14] F. Mosino, Storia linguistica della Calabria, I Marra Cosenza (1988) 91.
[15] G. Occhiato, Il Soccorpo in: La Cattedrale di Gerace, Cassa di risparmio di Calabria e Lucania, Effesette, Cosenza, 1986, pp. 84–99.
[16] G. Occhiato, Interpretazione della cripta del duomo normanno di Gerace in Calabria, in: Tomo Byzantion (Ed.), XLIX, 1979, pp. 314–362.
[17] P. Orsi, Le chiese basiliane della Calabria, Firenze Val. (1929).
[18] C. Genovese, I grandi monumenti per la valorizzazione dei beni culturali in Calabria. Il caso della Cattedrale di Gerace, in: Reuso: La cultura del restauro e della valorizzazione. Temi e problemi per un percorso internazionale di conoscenza, 2° Convegno Internazionale sulla documentazione, conservazione e recupero del patrimonio architettonico e sulla tutela paesaggistica, Alinea Editrice, Firenze, 2014.
[19] F. Mercuri, C. Cicero, N. Orazi, S. Paoloni, M. Marinelli, U. Zammit, Infrared thermography applied to the study of cultural heritage, Int. J. Thermophys. 36 (2015) 1189–1194, https://doi.org/10.1007/s10765-014-1645-x.
[20] A. Moropoulou, N.P. Avdelidis, M. Karoglou, E.T. Delegou, E. Alexakis, V. Keramidas, Multispectral applications of infrared thermography in the diagnosis and protection of built cultural heritage, Appl. Sci. 8 (2018) 284, https://doi.org/10.3390/app8020284.
[21] C. Meola, G.M. Carlomagno, Recent advances in the use of infrared thermography, Meas. Sci. Technol. 15 (2004) R27.
[22] C. Ibarra-Castanedo, J.R. Tarpani, X.P. Maldague, Nondestructive testing with thermography, Eur. J. Phys. 34 (2013) S91.
[23] A. Costanzo, M. Minasi, G. Casula, M. Musacchio, M.F. Buongiorno, Combined use of terrestrial laser scanning and ir thermography applied to a historical building, Sensors 15 (2015) 194–213, https://doi.org/10.3390/s150100194.
[24] C. Balaras, A. Argiriou, Infrared thermography for building diagnostics, Energy Build. 34 (2002) 171–183.
[25] C. Walker, I. Joosten, Introduction: analysis of cultural heritage, 655-655, Microsc. Microanal. 17 (5) (2011), https://doi.org/10.1017/S1431927611012062.
[26] C. Cardell, D. Benavente, J. Rodríguez-Gordillo, Weathering of limestone building material by mixed sulfate solutions, Charact. Stone Microstruct. React. Prod. Decay forms. Mater. Charact. 59 (2008) 1371–1385.
[27] A. Ali, Y.W. Chiang, R.M. Santos, X-ray diffraction techniques for mineral characterization: a review for engineers of the fundamentals, applications, and research directions, Minerals 12 (2022) 205, https://doi.org/10.3390/min12020205.
[28] J. Weiss. Handbook of Ion Chromatography, 4th ed..,, Wiley-VCH,, 2016. ISBN: 978-3-527-32928-1.
[29] A. Alvarez de Buergo, M.P. Lopez-Arce, R. Fort, Ion chromatography to detect salts in stone structures and to assess salt removal methods, EGU Gen. Assem. Conf. Abstr. vol. 14 (2012) 1757.
[30] P. Frongia, F. Di Gregorio, G. Piras, Indagini termografiche, trasformazioni architettoniche e degrado dei materiali nelle chiese del centro storico di Siliqua (Sardegna S-W), Boll. della Assoc. Ital. di Cartogr. (2013).
[31] G. Pappalardo, S. Mineo, D. Caliò, A. Bognandi, Evaluation of natural stone weathering in heritage building by infrared thermography, Heritage 5 (2022) 2594–2614, https://doi.org/10.3390/heritage5030135.
[32] R.L. Folk, Spectral subdivision of limestone types, Bull. Am. Assoc. Pet. Geol. 1 (1962) 62–84.

[33] R.J. Dunham, Classification of carbonate rocks according to depositional textures, Amer. Ass. Pet. Geol. (1962) 108–121.
[34] F. Bozzano, S. Martino, A. Prestininzi, Role of the geological setting on the stability conditions of the Gerace hill (Reggio CalabriaItaly), Ital. J. Geosciences 129 (2010) 280–296, https://doi.org/10.3301/IJG.2010.10.
[35] O. Petrucci, M. Polemio, Il dissesto della rupe di Gerace: patrimonio artistico e fattori idrogeologici di rischio, Convegno Geoben, Torino, 7–9 Giugno 2000.
[36] A.J. Matthew, A.J. Woods, C. Oliver, Spots before the eyes: New comparison charts for visual percentage estimation in archaeological material, in: A. Middleton, I. Freestone (Eds.), Recent developments in ceramic petrology, British Museum Research Laboratory, London, 1991, pp. 211–264.
[37] K. Elert, C. Rodriguez-Navarro, E.S. Pardo, E. Hansen, O. Cazalla, Lime mortars for the conservation of historic buildings, Stud. Conserv. 47 (1) (2002) 62–75, https://doi.org/10.1179/sic.2002.47.1.62.
[38] T. Schmid, P. Dariz, Raman microspectroscopic imaging of binder remnants in historical mortars reveals processing conditions, Heritage 2 (2019) 1662–1683, https://doi.org/10.3390/heritage2020102.
[39] S. Cuezva, J. Garcia-Guinea, A. Fernandez-Cortes, D. Benavente, J. Ivars, J.M. Galan, S. Sanchez-Moral, Composition, uses, provenance and stability of rocks and ancient mortars in a Theban Tomb in Luxor (Egypt), Mater. Struct. 49 (2016) 941–960, https://doi.org/10.1617/s11527-015-0550-5.
[40] M.A. Zicarelli, M.F. La Russa, M.F. Alberghina, S. Schiavone, R. Greca, P. Pogliani, M. Ricca, S.A. Ruffolo, A multianalytical investigation to preserve wall paintings: a case study in a hypogeum environment, Materials 16 (2023) 1380, https://doi.org/10.3390/ma16041380.
[41] David Hradil, Tomáš. Grygar, Janka Hradilová, Petr Bezdička, Clay and iron oxide pigments in the history of painting, Appl. Clay Sci. Volume 22 (Issue 5) (2003) 223–236, https://doi.org/10.1016/S0169-1317(03)00076-0.
[42] D. Hradil, J. Hradilová, P. Bezdička, Clay minerals in european painting of the mediaeval and baroque periods, Minerals 10 (2020) 255, https://doi.org/10.3390/min10030255.
[43] D. Hradil J. Hradilová P. Bezdička New criteria for classification of and differentiation between clay and iron oxide pigments of various origins 24–26 NovemberActa Artis. Acad., Proc. 3rd Interdiscip. ALMA Conf., Prague, Czech Repub. 2010 107 136.ISBN 978-80-87108-14-7.
[44] G. Vasco, A. Serra, D. Manno, G. Buccolieri, L. Calcagnile, A. Buccolieri, Investigations of byzantine wall paintings in the abbey of Santa Maria di Cerrate (Italy) in view of their restoration, Spectrochim. Acta A Mol. Biomol. Spectrosc. 239 (2020) 1386–1425.
[45] E. Cheilakou, M. Troullinos, M. Koui, Identification of pigments on Byzantine wall paintings from Crete (14th century AD) using non-invasive Fiber Optics Diffuse Reflectance Spectroscopy (FORS), J. Archaeol. Sci. 41 (2014) 541–555.
[46] M. Ricca, M.F. Alberghina, N.D. Houreh, A.S. Koca, S. Schiavone, M.F. La Russa, L. Randazzo, S.A. Ruffolo, Preliminary Study of the Mural Paintings of Sotterra Church in Paola (Cosenza, Italy), Materials 15 (2022) 3411, https://doi.org/10.3390/ma15093411.
[47] C. Crova, F. Miraglia, La termografia come strumento di indagine conoscitiva delle superfici architettoniche. Interventi e prospettive di ricerca, in Intervenire sulle superfici dell'architettura tra bilanci e prospettive, 34° Convegno Internazionale Scienza e Beni Culturali, Collana Scienza e Beni Culturali, 2018.
[48] S.J.C. Granneman, B. Lubelli, R.P.J. van Hees, Effect of mixed in crystallization modifiers on the resistance of lime mortar against NaCl and Na2SO4 crystallization, Construct. Build. Mater. 194 (2019) 62–70.
[49] A. Arnold K. Zehnder Monitoring Wall Paintings Affected by Soluble Salts Conserv. Wall Paint.: Proc. a Symp. Organ. Court. Inst. Art. Getty Conserv. Inst., Lond. 521 13–16 July 1987 103 132.
[50] L. Germinario, C.T. Oguchi, Underground salt weathering of heritage stone: lithological and environmental constraints on the formation of sulfate efflorescences and crusts, J. Cult. Herit. Volume 49 (2021) 85–93.
[51] T. Díaz Gonçalves, J. Delgado Rodrigues, M. Marinho Abreu, Evaluating the salt content of salt-contaminated samples on the basis of their hygroscopic behaviour: Part II: experiments with nine common soluble salts (July–September), J. Cult. Herit. Volume 7 (Issue 3) (2006) 193–200.
[52] I.S. Evans, Salt crystallization and rock weathering: a review, Rev. Géomorphol. Dyn. 19 (1970) 153–177.
[53] E.M. Winkler, Stone, in: Architectur, 1st ed.; Springer: Berlin/Heidelberg, Germany, 1994.
[54] A.S. Goudie, H.A. Viles. Salt Weathering Hazard, 1st ed..,, Wiley,, London, UK, 1997.
[55] C. Rodriguez-Navarro, E. Doehne, Salt weathering: influence of evaporation rate supersaturation and crystallization pattern, Earth Surf. Process. Landf. 24 (1999) 191–209.